Influence of Thermal Process on Physical Properties of ZnO Films Prepared by Spray Pyrolysis

O. Gencyilmaz[a,*], F. Atay[b] and I. Akyuz[b]

[a]Department of Physics, CankırıKaratekin University, Cankırı, Turkey

[b]Department of Physics, Eskisehir Osmangazi University, Eskisehir, Turkey

(Received January 6, 2014; in final form July 22, 2014)

ZnO films were deposited on glass substrates by ultrasonic spray pyrolysis technique at a substrate temperature of 300 ± 5 °C. All of the films have been annealed at 500 °C temperature for different time (1, 2, and 3 h) to improve the optical, electrical and surface properties. The effect of annealing time on the films of physical properties has been investigated. UV-Vis spectrophotometer has been used for transmittance measurements. Also, band gap values of the films have been determined by optical method. Atomic force microscopy has been used to have information the surface morphology and roughness values of the films. Thicknesses, refractive index and extinction coefficient values of the films have been determined by spectroscopic ellipsometry technique. The electrical conduction mechanisms and resistivity of the films were investigated using two probe technique. After all the investigations it was concluded that annealing time has a dramatic effect especially on the surface, optical properties and electrical resistivity values of ZnO films. From the results of these investigations, the application potential of the films for solar cell devices as transparent electrode was searched.

DOI: 10.12693/APhysPolA.126.1331

PACS: 81.05.Dz, 78.66.Hf, 73.61.Ga, 68.37.Ps

1. Introduction

ZnO is one of the few metal oxides which can be used as a transparent conducting oxide in many applications [1]. Thin films of ZnO have been used for a variety of applications such as display devices, heat mirror, photovoltaics and electronic transducers because of their high stability, electrical conductivity and transparency [2, 3]. On the other hand, this oxide has been applied in light emitting diodes [4], photo detectors [5], piezoelectric cantilever [6], gas sensors [7], buffer layer in CIGS solar cells [8], and dye sensitized solar cells (DSSC) [9]. ZnO is an attractive oxide semiconductor which has wide band gap (3.3 eV at room temperature) and direct band transition. ZnO thin films may be prepared by different techniques including metal–organic chemical vapor deposition [10, 11], magnetron sputtering [12, 13] and chemical spray pyrolysis [14–17]. Among these methods, spray pyrolysis is an attractive method to obtain thin films of ZnO, since it is low cost, simple method and it does not require a high vacuum apparatus.

Thermal annealing is widely used to improve crystal quality, which affects electrical, optical and structural properties by reducing defects in materials. The annealing process, especially at the surface regions, influence the structure of the material. Detailed the effects of annealing processes on surfaces properties of ZnO films can be investigated by analysis of surface properties such as surface roughness or optical properties by spectroscopic ellipsometry. Spectroscopic ellipsometry technique is a very sensitive measurement technique that uses polarized light to characterize thin films, surfaces, and material microstructure. There is almost no study about effect of annealing time on physical properties of ZnO films in the literature. Aim of this work is to see the effect of annealing time on the optical, surface and electrical properties of ZnO films.

2. Experimental details

ZnO films were grown onto glass substrates (1×1 cm^2) at 300 ± 5 °C temperatures by spray pyrolysis technique. The spray solution was prepared from a mixture 0.1 M zinc acetate [$Zn(CH_3COO)_2 \cdot 2H_2O$] and distilled water. Totally, 100 ml of solution was used and sprayed for 20 min. The solution flow rate was kept at 5 ml/min and controlled by a flowmeter. Details of the spray pyrolysis technique were published elsewhere [18, 19]. After spraying process, the deposited ZnO films were annealed in ambient air at 500 °C temperature for different time (1, 2, and 3 h).

Optical transmission measurements were performed with a Perkin Elmer Lambda 2S UV-VIS spectrophotometer over the wavelength range of 300–900 nm. The thicknesses, refractive index and extinction coefficient values of ZnO films were obtained from spectroscopic ellipsometry (SE) measurements.

PHE-102 Spectroscopic Ellipsometer (spectral range 250–2300 nm) was used to determine the Δ parameters, refractive indices (n), extinction coefficient (k) and thicknesses (t) of the films. The Cauchy–Urbach dispersion model was used to fit the experimental Δ parameters. This model is a modified type of Cauchy model. In the Cauchy-Urbach dispersion model, the refractive index $n(\lambda)$ and the extinction coefficient $k(\lambda)$ as a function of the wavelength are given by

*corresponding author; e-mail: eren_o@hotmail.com

$$n(\lambda) = A + \frac{B}{\lambda^2} + \frac{C}{\lambda^4}, \tag{1}$$

$$k\lambda = \alpha \exp\beta \left[12400\left(\frac{1}{\lambda} - \frac{1}{\gamma}\right)\right], \tag{2}$$

where A, B, C, α, β and γ are model parameters [20, 21]. The Cauchy–Urbach model may be used for samples with low absorption. For this reason, the measurements were taken between the wavelength ranges of 1200–1600 nm where the films have low absorption. For the samples having depolarization effect, the incident angle is an important factor. This will affect the intensity and phase of the reflected light which then goes to the analyzer. Five different incident angles (55°, 60°, 65°, 70°, 75°) were tried to take the measurements. The best angle was determined to be 65° using experimental Δ spectra. Then, the parameters (A, B, C, α, β) related to the Cauchy–Urbach model were determined.

The surface morphology was studied by using Park System XE 70 model atomic force microscopy. The measurements were taken in non-contact mode, $\approx$ 300 kHz frequency and 0.75 Hz scan rate in air at room temperature. A silicon cantilever which has a spring constant of 40 N/m was used. Also, average (R_a) roughness values were obtained using XEI version 1.7.1 software. All the images were taken from an area of 2×2 μm^2. The roughness values belong to all scanned area.

The electrical properties of the films were investigated by using a two-probe system, Fluke Voltage/Current Calibrator Model 382a and Keithley 619 Electrometer.

3. Results and discussion

Ellipsometric angles Δ were investigated by spectroscopic ellipsometry. The optical constants (n), (k) and the thickness of ZnO films were investigated. Ellipsometric data of ZnO films were fitted according to the Cauchy–Urbach exponential model and reflection spectra taken from spectroscopic ellipsometry. The technique itself is based on the fact that linearly polarised light beam, which is cast on the sample surface, is reflected and its polarization state is changed. The ellipsometric angles are denoted by Δ, which are related to complex reflectance ratio ρ:

$$\rho = \frac{\widetilde{R}_{\mathrm{P}}}{\widetilde{R}_{\mathrm{S}}} = \tan\Psi \mathrm{e}^{\mathrm{i}\,\Delta}, \tag{3}$$

where $\widetilde{R}_{\mathrm{P}}$ and $\widetilde{R}_{\mathrm{S}}$ are complex reflection coefficients which are parallel and perpendicular to the plane of incidence, respectively [22]. The measured SE data for Δ of ZnO films on glass substrates in the wavelength range of 1200–1600 nm is shown in Fig. 1. The experimental data were analyzed by using the Cauchy–Urbach exponential model. In spite of a good correlation provided between model and experimental data, there are some small deviations on fitted Δ values. We think that the possible reason may be the roughness, grain boundaries, and morphology of the sample.

Fitting the experimental ellipsometric spectra of Δ allowed the determination of the film thickness (t), spectra of refractive index (n) and extinction coefficient (k) of all films. The thickness values of ZnO films and ellipsometric data are given in Table I. The thickness values of the films were varied from 259 to 276 nm and values of MSE were fairly low. When the ZnO films were annealed for more than 2 h, thickness of films was found to increase.

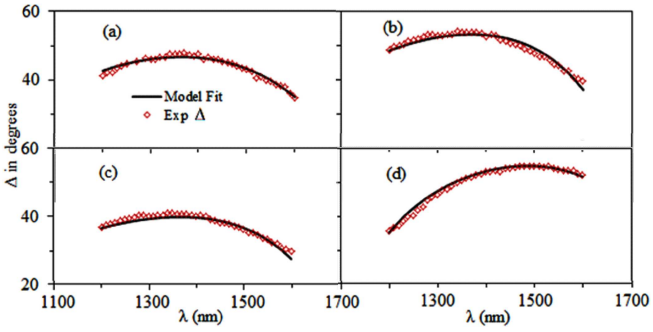

Fig. 1. SE spectra of as-deposited at 300 °C and annealed ZnO films at 500 °C: (a) as deposited, (b) annealed for 1 h, (c) annealed for 2 h, (d) annealed for 3 h.

TABLE I

Thickness and ellipsometric data values of ZnO films, as a function of annealed time, obtained by a spectroscopic ellipsometry study.

Material	t [nm]	A_n	B_n [nm^2]	C_n [nm^4]	α	β [nm]	MSE
as deposited	259	1.97	0.04	0.01	0.048	0.074	0.43
annealed for 1 h	236	2.04	0.01	0.06	0.086	0.036	0.89
annealed for 2 h	243	2.01	0.01	0.01	0.075	0.042	0.81
annealed for 3 h	276	1.88	0.29	0.05	0.124	0.063	0.6

Optical properties of unannealed and annealed ZnO films were investigated with the help of transmission spectra in the UV–Visible region and recorded in the range 300-900 nm. Figure 2 shows the optical transmission spectra of ZnO films prepared on the glass substrates at a temperature of 300 °C followed by annealing at various time (1, 2, 3 h). It is clear from Fig. 2 that annealing the samples caused an increase in transmittance values. Decrease of thickness may be a reason for the increase in transmittance values of samples annealed for 1 and 2 h. Similar results have been reported by Nadarajah et al. [23]. There is another effect of annealing on the optical properties of ZnO films. Samples annealed for 1 and 2 h have shown interference fringes in transmittance spectra. It is well known that thin films with uniform and continuous surfaces may probably show these fringes. So, we think that improved surface texture and decreasing roughness values of the samples annealed for 1 and 2 h caused interference fringes to occur in transmittance spectra.

Annealing process has also been an important effect on the surface properties of ZnO films as can be seen from our atomic force microscopy (AFM) images (Fig. 3).

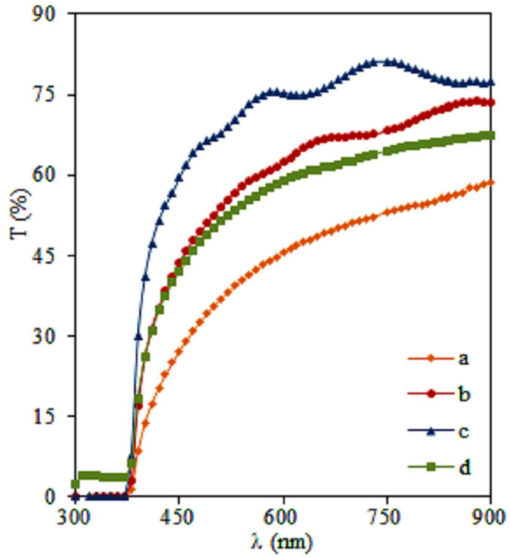

Fig. 2. UV-Vis transmittance spectra of as-deposited at 300 °C and annealed ZnO films at 500 °C: (a) as deposited, (b) annealed for 1 h, (c) annealed for 2 h, (d) annealed for 3 h.

So, the improvement of the transmittance for annealed samples could be related to decrease in optical scattering processes after annealed. This kind of effect has been reported by Senadım et al. [24], Ma et al. [25] and Mahmood et al [26].

ZnO film that is annealed during 2 h has the highest optical transmittance ($\approx 86\%$). The high annealing time above 2 h leads to decrease of the transmittance in the visible range. It suggests that annealing ambient has a great influence on the optical transmittance of ZnO film. Aly et al. [27] found that thermal annealing in air could improve the optical transmittance of ZnO films, attributing to the oxygen reaction with ZnO. In addition, we can see from Fig. 2 that the absorption edge has been changed after the annealing. The sharp absorption edges can be clearly observed with the increases of the annealing time as shown in the inset of Fig. 2. In addition, sharp absorption edges can be clearly observed and shift to the shorter wavelength as the increases of the annealing time (below 3 h) as shown in the inset of Fig. 2. We think that our as-grown sample has deformation and defects near band edges. Annealing may probably lead to decrease of such deformations and resulted with a sharper absorption edge. This will also cause the optical band values to increase as can be seen from Fig. 4.

Reflection (R) spectra of ZnO films are shown in Fig. 5. It was determined that the average reflection value of films is below 6% in the visible region of the spectrum. Especially, low reflectance value of long duration annealed film (3 h) makes this film a promising material for photovoltaic applications as window material or front contact.

Figure 6 shows the dependence of the refractive indices of ZnO film on the wavelength. It can be seen that the refractive index increases while increasing annealing time. When we look at Fig. 6, refractive indices of all films are almost constant with increasing wavelength. This is an expected result for this wavelength range because all films are nearly transparent in this region. There is a little decrease in refractive index value for ZnO which is annealed for 3 h. Also, refractive index values of the samples are nearly constant ($\approx 1.95-2.15$) at long wavelengths.

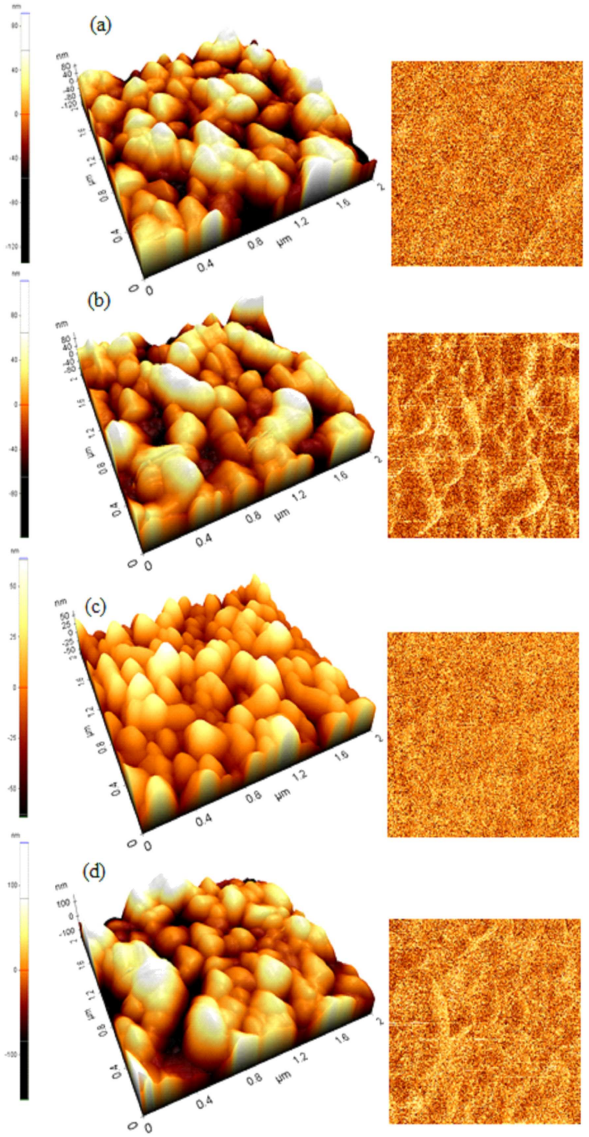

Fig. 3. AFM images of ZnO films for as-deposited at 300 °C and annealed ZnO films at 500 °C: (a) as deposited, (b) annealed for 1 h, (c) annealed for 2 h, (d) annealed for 3 h.

Figure 7 shows the extinction coefficients (k) of ZnO films which are derived from model fitting the experimental spectroscopic ellipsometric data. It can also be seen that the extinction coefficient increases when increasing the annealing time.

The optical band gap energy E_g was calculated from the absorption spectra. We used the variation of the ab-

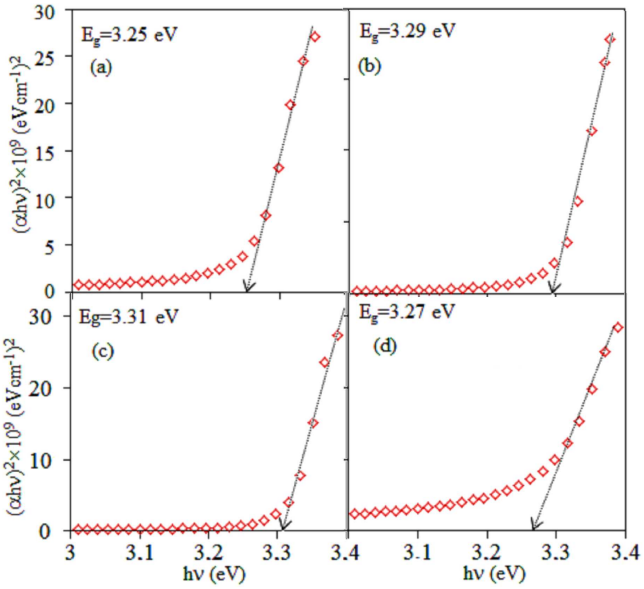

Fig. 4. $(\alpha h\nu)^2$ versus $(h\nu)$ plots of ZnO films for as-deposited at 300 °C and annealed ZnO films at 500 °C: (a) as deposited, (b) annealed for 1 h, (c) annealed for 2 h, (d) annealed for 3 h.

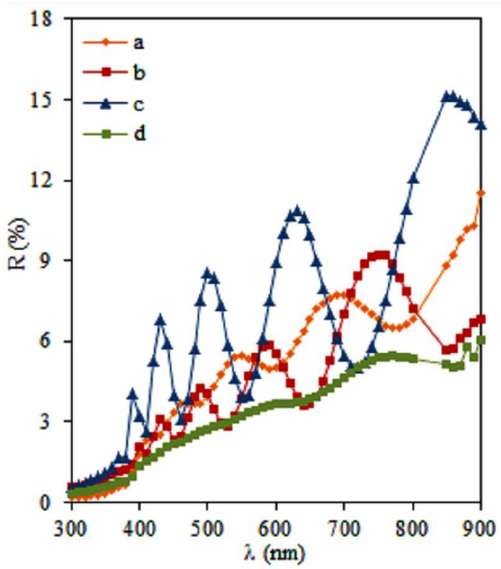

Fig. 5. Reflection (R) spectra of as-deposited at 300 °C and annealed ZnO films at 500 °C: (a) as deposited, (b) annealed for 1 h, (c) annealed for 2 h, (d) annealed for 3 h.

sorption coefficient (α) with photon energy, the relation

$$\alpha h\nu = A(h\nu - E_g)^n, \tag{4}$$

where A is a constant, E_g the band gap of the material and n is a constant which determines type of the optical transition ($n = 1/2$ for allowed direct transitions and $n = 2$ for allowed indirect transitions). Here $n = 1/2$, corresponding to the allowed direct transition [28]. The optical gap was determined from the plot of $(\alpha h\nu)^2$ versus photon energy.

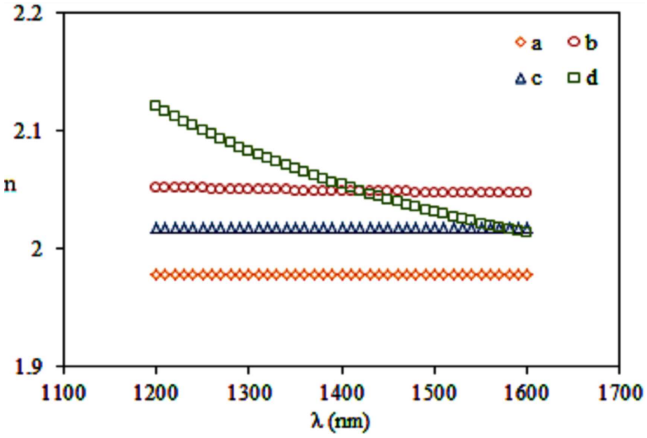

Fig. 6. Refractive index (n) spectra of as-deposited at 300 °C and annealed ZnO films at 500 °C: (a) as deposited, (b) annealed for 1 h, (c) annealed for 2 h, (d) annealed for 3 h.

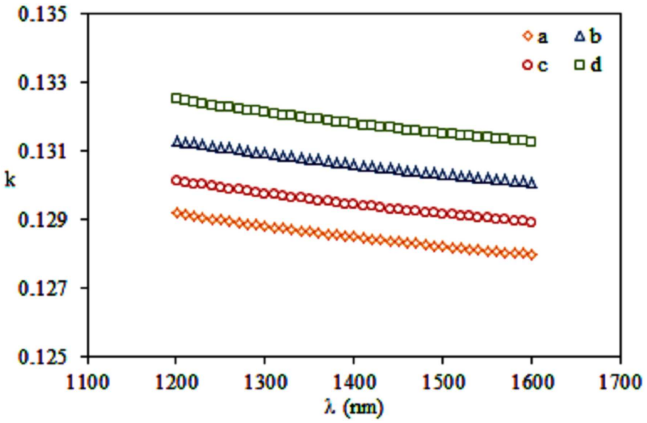

Fig. 7. Extinction coefficient (k) spectra of as-deposited at 300 °C and annealed ZnO films at 500 °C: (a) as deposited, (b) annealed for 1 h, (c) annealed for 2 h, (d) annealed for 3 h.

Figure 4 shows the plots of $(\alpha h\nu)^2$ versus $(h\nu)$ for various ZnO films. Extrapolation of the linear portions of the plots onto the energy axis was used to estimate the band gap values. The extrapolated values of the optical energy gap E_g are between 3.2 and 3.3 eV for the samples that were as grown and annealed for 1, 2, 3 h, respectively. It can be seen that the optical absorption edge exhibits slight blue shift with increasing annealing time below 3 h. However, it exhibits evident red shift at 3 h of the annealing time. Xuea et al. [29] have also reported a blue shift and a red shift with annealing process in their studies.

As we mentioned before, the shifts of the optical absorption edge may be attributed to the decreasing defects and deformation of the ZnO films with increasing annealing time. Also, this may be due to the extension of electronic states of the impurity phase, precipitates and clusters, into the band gap of ZnO. Also, all films were found to be direct band gap materials, which is a desired

property for photovoltaic solar cell applications.

It is known that the absorption coefficient near the band edge shows an exponential dependence on photon energy [30],

$$\alpha(\nu) = \alpha_0 \exp(h\nu/E_0), \tag{5}$$

where E_0 is the Urbach energy which corresponds to the width of the band tail and can be evaluated as the width of the localized states. α_0 is a constant. Thus, a plot of $\ln[\alpha(\lambda)]$ versus photon energy should be linear and Urbach energy can be obtained from the slope.

The $\ln[\alpha(\lambda)]$ versus photon energy plots for the film annealed at different hours are shown in Fig. 8. The Urbach energy was calculated from the reciprocal gradient of the linear portion of these curves.

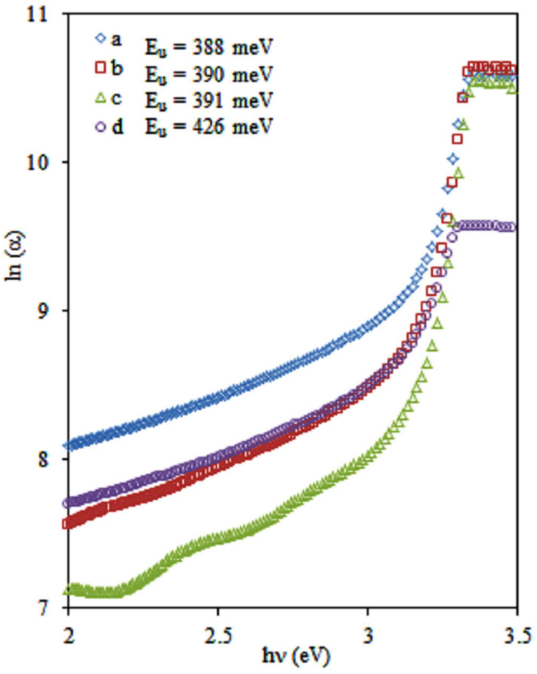

Fig. 8. The Urbach plots of for as-deposited at 300 °C and annealed ZnO films at 500 °C: (a) as deposited, (b) annealed for 1 h, (c) annealed for 2 h, (d) annealed for 3 h.

Both Urbach energy and optical band gap alteration is shown in Fig. 9. The Urbach energy increases slightly with increase of the annealing time. After that, the width of the band tail increases with increase of the annealing time above 2 h. In this long annealing time, we think that thermal induced structural disorder of the film increases with the increase of annealing time, which leads to a degradation of the ZnO film. These results fundamentally agree with the analysis results of the shift of the optical absorption edge.

AFM has been used to have information on the surface morphology and roughness values of the films. The AFM images of the films are shown in Fig. 3. Figure 3 shows that there are different regions on the surface of as-grown ZnO films with various heights. There are randomly dis-

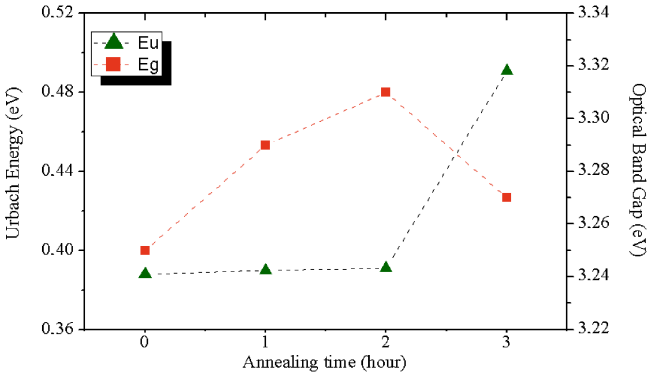

Fig. 9. Urbach energy and optical band gap of the ZnO film as a function of the annealing time.

tributed mount type formations and regions with different height and width. Annealing caused that the films have different surface morphology with decrease of height and width. Also, cluster-like formations and discontinuity on film surface need to be noted. But, with increase of annealing time, surface texture of the films starts to change. Especially the sample annealed for 2 h has a uniform surface with distinguishable particles. This granular structure may probably have positive effect on the optical properties of this sample, as we have mentioned before. We can conclude that annealing process has a dramatic effect on the surface properties of the films, especially for the sample annealed for 2 h. Similar effect has been reported by Nehru et al. [31]. Consequently, the surface morphology of ZnO films that were annealed for 2 h has the best granular structure.

Annealing process has also changed the roughness values of ZnO films. Average (R_a) roughness values of the ZnO films were examined and these values are given in Table II. It is clear that annealing process affected the roughness values of ZnO films. The roughness value of the film slightly decreases with the annealing that has been reported in the literature [31, 32]. We think that this decrease is manly related to the surface combination and surface form. Also, the average roughness (R_a) values of the films are between 30–63 nm which are lower than that of the results of the report given by Nehru et al. [31]. Samples annealed for 1 and 2 h have lower R_a values than other samples. Annealing may probably cause the atoms to migrate energetically favorable sites and cause a uniform distribution on the surface. As we have mentioned before, this type of texture caused interference fringes in transmittance spectra to occur.

The $I-V$ characteristics of films were investigated and the electrical resistivity of ZnO films which were unannealed and annealed at 1, 2, and 3 h was measured. The $I-V$ plots of all films in these conditions are shown in Fig. 10. For the ZnO films, the current changed in the 10–100 V voltage range. Also, the resistivity values of all films were calculated and were presented in Table III. It was seen that the resistivity of ZnO films decrease with increase of annealing time. A similar behavior with

TABLE II

The average roughness values of the unannealed and annealed ZnO films.

Material	R_a [nm] (2×2 μm^2)
as deposited	63
annealed for 1 h	46
annealed for 2 h	30
annealed for 3 h	59

the change in electrical resistivity has been reported by Nunes et al. [33], Lee and Park [34] and Ma and Shim in their studies [35].

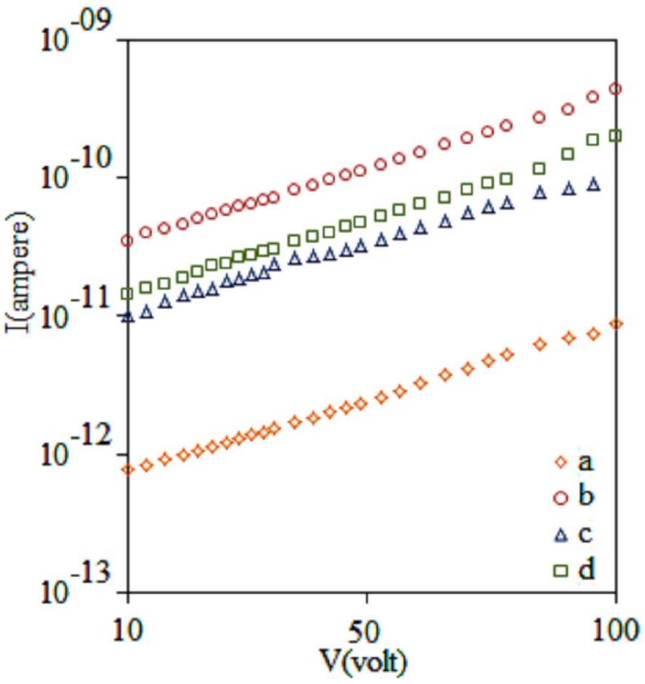

Fig. 10. I–V plots of as-deposited at 300 °C and annealed ZnO films at 500 °C: (a) as deposited, (b) annealed for 1 h, (c) annealed for 2 h, (d) annealed for 3 h.

TABLE III

Electrical resistivity values of ZnO films.

Material	Electrical resitivity [Ωcm]
as deposited	218
annealed for 1 h	18.5
annealed for 2 h	27.9
annealed for 3 h	11.1

We think that the reason for this annealing of the ZnO film can lead to desorption and chemisorption of oxygen molecules which are chemisorbed in the film both at grain boundaries and also on the surface. Because the resistivity behavior on annealing of films at different ambient temperature and time can be explained on the basis of chemisorption and desorption of oxygen at grain boundaries of polycrystalline films [36]. Annealing process may cause the desorption of oxygen from these regions. We think that this will not only lower the potential barrier but also increase carrier concentration. In addition, it is well known that oxygen tends to site at grain boundaries in polycrystalline films. These oxygen spaces may produce potential barrier for charge carriers [37–39]. Finally, these will cause the resistivity values of annealed ZnO films to decrease, as shown in Table III.

4. Conclusion

The ZnO thin films have been fabricated by spray pyrolysis method at 300 ± 5 °C substrate temperature and annealed for 1, 2, and 3 h. Effects of the annealing time on optical, surface and electrical properties of ZnO thin films were investigated. Optical properties of the films were analyzed by transmittance, absorbance spectra and the optical method was used for determining the band gaps of the films. The optical constants (n), (k) and the thickness of ZnO films were fitted according to the Cauchy–Urbach exponential model by reflection spectra taken from spectroscopic ellipsometry. A good fit is found between model and experimental data but there are some declinations on fitted Δ values. Also, the optical band gap values between 3.2 and 3.3 are changed. The highest transmittance was observed in 2 h annealing. As shown from Fig. 3, maximum reduction in refractive index has been at 3 h annealing. The surface morphology of ZnO films were investigated by using atomic force microscopy (AFM) images; also these pictures showed grain boundaries and roughness values of the films. The surface morphology characterizations of ZnO films with results of spectroscopic ellipsometry are compatible. The electrical resistivity values were calculated using the $I-V$ graphics. The electrical resistivity of ZnO films decrease with increase of annealing time. As shown from Table III, minimum electrical resistivity of ZnO films has been at 3 h annealing. Consequently, 1 and 2 h annealing ZnO films can be used as transparent electrode in photovoltaic solar cell. However, 3 h annealing ZnO film can be used in different applications.

References

[1] R.G. Gordon, *MRS Bull.* **25**, 52 (2000.

[2] T.H. Aeugle, H. Bialas, K. Heneka, W. Pleyer, *Thin Solid Films* **201**, 293 (1991).

[3] S. Matsuushima, D. Ikeda, K. Kobayashi, G. Okada, *Chem. Lett.* **2**, 323 (1992).

[4] Y. Chen, D. Bagnall, T. Yao, *Mater. Sci. Eng. B* **75**, 190, (2000).

[5] K.J. Chen, F.Y. Hung, S.J. Chang, S.J. Young, *J. Alloys Comp.* **479**, 674 (2009).

[6] S.H. Lee, S.S. Lee, J.J. Choi, J.U. Jeon, K. Ro, *Microsystem Technol.* **11**, 416 (2005).

[7] J. Xua, Q. Pan, Y. Shun, Z. Tian, *Sensors Actuat. B* **66**, 277, (2007).

[8] A. Romeo, D.L. Bätzner, H. Zogg, A.N. Tiwari, *MRS Symp. Proc.* **668**, H3.3 (2001).

[9] T.W. Hamann, A.B.F. Martinson, J.W. Elam, M.J. Pellin, J.T. Hupp, *Adv. Mater.* **20**, 1560 (2008).

[10] K. Haga, T. Suzuki, Y. Kashiwaba, H. Watanabe, B.P. Zhang, Y. Segawa, *Thin Solid Films* **433**, 131 (2003).

[11] A. Martin, J.P. Espinos, A. Justo, J.P. Holgado, F. Yubero, A.R. Gonzatez-Elipe, *Surf. Coat. Technol.* **289**, 151 (2002).

[12] H.F. Winters, P. Sigmund, *J. Appl. Phys.* **45**, 4760 (1974).

[13] G. Fang, D. Li, B.-L. Yao, *Vacuum* **68**, 363 (2003).

[14] J. San, T. Yang, G. Du, H. Liang, J. Bian, L. Hu, *Appl. Surf. Sci.* **253**, 2066 (2006).

[15] E. Bacaksiz, M. Parlak, M. Tomakin, A. Ozcelik, M. Kiraz, M. Altunbas, *J. Alloys Compd.* **466**, 447 (2008).

[16] M. Miki-Yoshida, F. Paraguay-Delgado, W. Estrada-Lopez, *Thin Solid Films* **376**, 99 (2000).

[17] J.M. Bian, X.M. Li, X.D. Gao, W.D. Yu, L.D. Chen, *Appl. Phys. Lett.* **84**, 541 (2004).

[18] J. Nolly, K.K. Abdullah, K.P. Vijayakumar, *Phys. Lett., Spec. Issue* **22**, (2000).

[19] F. Atay, S. Kose, V. Bilgin, I. Akyuz, *Mater. Lett.* **57**, 3461 (2003).

[20] M. Khoshman Jebreel, E. Kordesch Martin, *J. Non-Cryst. Solids* **351**, 3334 (2005).

[21] F. Atay, I. Akyuz, S. Kose, E. Ketenci, V. Bilgin, *J. Mater. Sci. Mater. Electron.* **22**, 492 (2011).

[22] Y. Yang, X.W. Sun, B.J. Chen, C.X. Xu, T.P. Chen, C.Q. Sun, B.K. Tay, Z. Sun, *Thin Solid Films* **510**, 95 (2006).

[23] K. Nadarajah, C.Y. Chee, C.Y. Tan, *J. Nanomater.* **2013**, ID 146382 (2013).

[24] E. Senadım, H. Kavak, R. Esen, *J. Phys. Condens. Matter* **18**, 6391 (2006).

[25] S.Y. Ma, X.H. Yang, X.L. Huang, A.M. Sun, H.S. Song, H.B. Zhu, *J. Alloys Comp.* **566**, 9 (2013).

[26] A. Mahmood, A. Nadeem, Q. Raza, Taj Muhammad Khan, M. Mehmood, M.M. Hassan, N. Mahmood, A. Mahmood, *Phys. Scr.* **82**, 065801 (2010).

[27] S.A. Aly, N.Z. El Sayed, M.A. Kaid, *Vacuum* **61**, 1 (2001).

[28] M. Kruns, E. Mellikov, *Thin Solid Films* **270**, 33 (1995).

[29] S.W. Xuea , X.T. Zu , W.L. Zhou, H.X. Deng, X. Xiang, L. Zhang, H. Deng, *J. Alloys Comp.* **448**, 21 (2008).

[30] V.R. Shinde, T.P. Gujar, C.D. Lokhande, R.S. Mane, S.H. Han, *Mater. Chem. Phys.* **96**, 326 (2006).

[31] L.C. Nehru, M. Umadevi, C. Sanjeeviraja, *Int. J. Mater. Eng.* **2**, 12 (2012).

[32] S.Y. Chu, W. Water, J.T. Liaw, *J. Europ. Ceram. Soc.* **23**, 1593 (2003).

[33] P. Nunes, E. Fortunato, R. Martins, *Int. J. Inorg. Mater.* **3**, 1125 (2001).

[34] J.H. Lee, B.O. Park, *Mater. Sci. Eng. B* **106**, 242 (2004).

[35] T.Y. Ma, D.K. Shim, *Thin Solid Films* **410**, 8 (2002).

[36] S. Major, A. Banerjee, K.L. Chopra, *Thin Solid Films* **122**, 31 (1984).

[37] Q.H. Li, Q. Wan, Y.X. Liang, T.H. Wang, *Appl. Phys. Lett.* **84**, 4556 (2004).

[38] B.L. Zhu, D.W. Zeng, J. Wu, W.L. Song, C.S. Xie, *J. Mater. Sci. Mater. Electron.* **14**, 521 (2003).

[39] B.L. Zhu, C.S. Xie, J. Wu, D.W. Zeng, A.H. Wang, X.Z. Zhao, *Mater. Chem. Phys.* **96**, 459 (2006).